CFTR: The Nucleotide Binding Folds Regulate the Accessibility and Stability of the Activated State

DANIEL J. WILKINSON,* MONIQUE K. MANSOURA,‡ PETER Y. WATSON,* LISA S. SMIT,‡ FRANCIS S. COLLINS,‡§‖¶ and DAVID C. DAWSON*

From the Departments of *Physiology, ‡Human Genetics, and §Internal Medicine, and the Bioengineering Program, University of Michigan, Ann Arbor, Michigan 48109; the ‖Howard Hughes Medical Institute, Ann Arbor, Michigan 48109; and the ¶National Center for Human Genome Research, Bethesda, Maryland 20892

ABSTRACT The functional roles of the two nucleotide binding folds, NBF1 and NBF2, in the activation of the cystic fibrosis transmembrane conductance regulator (CFTR) were investigated by measuring the rates of activation and deactivation of CFTR Cl^- conductance in *Xenopus* oocytes. Activation of wild-type CFTR in response to application of forskolin and 3-isobutyl-1-methylxanthine (IBMX) was described by a single exponential. Deactivation after washout of the cocktail consisted of two phases: an initial slow phase, described by a latency, and an exponential decline. Rate analysis of CFTR variants bearing analogous mutations in NBF1 and NBF2 permitted us to characterize amino acid substitutions according to their effects on the accessibility and stability of the active state. Access to the active state was very sensitive to substitutions for the invariant glycine (G551) in NBF1, where mutations to alanine (A), serine (S), or aspartic acid (D) reduced the apparent on rate by more than tenfold. The analogous substitutions in NBF2 (G1349) also reduced the on rate, by twofold to 10-fold, but substantially destabilized the active state as well, as judged by increased deactivation rates. In the putative ATP-binding pocket of either NBF, substitution of alanine, glutamine (Q), or arginine (R) for the invariant lysine (K464 or K1250) reduced the on rate similarly, by two- to fourfold. In contrast, these analogous substitutions produced opposite effects on the deactivation rate. NBF1 mutations destabilized the active state, whereas the analogous substitutions in NBF2 stabilized the active state such that activation was prolonged compared with that seen with wild-type CFTR. Substitution of asparagine (N) for a highly conserved aspartic acid (D572) in the ATP-binding pocket of NBF1 dramatically slowed the on rate and destabilized the active state. In contrast, the analogous substitution in NBF2 (D1370N) did not appreciably affect the on rate and markedly stabilized the active state. These results are consistent with a hypothesis for CFTR activation that invokes the binding and hydrolysis of ATP at NBF1 as a crucial step in activation, while at NBF2, ATP binding enhances access to the active state, but the rate of ATP hydrolysis controls the duration of the active state. The relatively slow time courses for activation and deactivation suggest that slow processes modulate ATP-dependent gating.

INTRODUCTION

The cystic fibrosis transmembrane conductance regulator (CFTR) is a membrane protein that functions as a Cl^--selective ion channel (Anderson et al., 1991*b*; Bear et al., 1992). Analysis of the primary amino acid sequence of CFTR (Riordan et al., 1989) provided evidence for three cytosolic domains that are likely to be involved in the regulation of CFTR function: the R domain, which contains multiple consensus sites for phosphorylation by cAMP-dependent protein kinase (PKA), and two nucleotide binding folds (NBF1 and NBF2), both containing regions with high sequence similarity to a family of proteins known to bind and hydrolyze ATP. This predicted domain topology foreshadowed functional studies of CFTR demonstrating that activation of CFTR Cl^- channels requires phosphorylation at one or more sites as well as the binding and hydrolysis of ATP (Anderson et al., 1991*a*; Berger et al., 1991; Cheng et al., 1991; Tabcharani et al., 1991; Bear et al., 1992; Carson and Welsh, 1993; Baukrowitz et al., 1994; Hwang et al., 1994).

The two NBFs of CFTR exhibit sequence similarity

Address correspondence to David C. Dawson, Ph.D., Department of Physiology, Box 0622, University of Michigan Medical School, Ann Arbor, MI 48109.

J. GEN. PHYSIOL. © The Rockefeller University Press • 0022-1295/96/01/103/17 $2.00
Volume 107 January 1996 103–119

that is sufficient to allow the identification of analogous residues in the two domains (Riordan et al., 1989; Gregory et al., 1991). In a previous study (Smit et al., 1993), we compared the effects of analogous mutations in NBF1 and NBF2 on the steady state activation kinetics of CFTR, assayed by determining the dose–response for the activation of cAMP-dependent Cl^- currents by the phosphodiesterase inhibitor, IBMX, in the presence of forskolin, an activator of adenylate cyclase. The results suggested that both NBFs function in the activation of CFTR, but in different ways. Mutations of an invariant glycine in either NBF1 (G551) or NBF2 (G1349) produced similar reductions in the sensitivity to activating conditions. In contrast, mutations in the putative ATP-binding pockets of the two NBFs produced opposite results, a reduction in sensitivity for mutations in NBF1 (K464Q, D572N) and an increase in sensitivity for the analogous mutations in NBF2 (K1250Q, D1370N).

In the studies described here, we characterized the roles of the two NBFs in the opening and closing of CFTR Cl^- channels by measuring the rates of activation and deactivation of Cl^- conductance associated with wild-type CFTR and mutants bearing single amino acid substitutions in NBF1 or NBF2. Using a two-state model for activation, we examined the roles of each NBF in regulating access to the activated state (on rate) and in determining the stability of the activated state (off rate). The results are compatible with a scheme in which the two NBFs interact to effect activation of CFTR in a manner such that ATP binding and hydrolysis at NBF1 is critical for entering the active state, but ATP binding at NBF2 also contributes to this process. Both NBFs appear to influence the stability of the active state, but in opposite ways, NBF1 stabilizing and NBF2 destabilizing the conducting conformation. Some of this work has been presented in abstract form (Wilkinson et al., 1993, 1994).

MATERIALS AND METHODS

Site-directed Mutagenesis, Plasmid Construction, and RNA Synthesis

CFTR mutants were generated as described previously (Smit et al., 1993) by cloning Sph I–Sac I fragments of the CFTR cDNA into the pSelect vector (Promega Corp., Madison, WI) and performing site-directed mutagenesis, using oligonucleotides that corresponded to the desired mutations. A 1.7-kb fragment of the cDNA that includes the Walker A region of NBF1 was used to make mutations at lysine 464, while a 3.0-kb fragment that includes glycine 551 and the Walker B region of NBF1 as well as glycine 1349 and the Walker A and B regions of NBF2 was used to make mutations at those sites. Mutations were verified by sequencing, and the mutated fragments were transferred into a full-length CFTR cDNA construct (Drumm et al., 1990) in pBluescript (Stratagene Inc., La Jolla, CA). RNA was synthesized by in vitro transcription, as described previously (Drumm et al., 1991), then suspended in diethylpyrocarbonate-treated water for injection.

Oocytes and RNA Injection

Female toads (*Xenopus laevis*, Xenopus-I, Inc., Ann Arbor, MI) were anesthetized by immersion in ice water containing 3-aminobenzoic acid ethyl ester (Tricaine, 3 mg/ml, Sigma Chemical Co., St. Louis, MO), and oocytes were removed through a small abdominal incision. The follicular membranes were removed by blunt dissection after incubation for 2–6 h in a nominally Ca^{2+}-free denuding solution containing 82.5 mM NaCl, 2 mM KCl, 1 mM $MgCl_2$, 5 mM HEPES (pH 7.5), and 2.5 mg/ml collagenase (Gibco Laboratories, Grand Island, NY). Defolliculated oocytes were kept overnight in a modified Barth's solution (MBSH) containing 88 mM NaCl, 1 mM KCl, 2.4 mM $NaHCO_3$, 0.82 mM $MgSO_4$, 0.33 mM $Ca(NO_3)_2$, 0.41 mM $CaCl_2$, 10 mM HEPES, and gentamicin sulfate (150 mg/liter), then injected with 0.1–15 ng of RNA (50 nl volume) using a microinjector (Drummond Scientific Co., Broomhall, PA). Injected oocytes were incubated at 19°C in 96-well microtiter plates containing MBSH, with one oocyte per well. Injection pipettes were pulled from glass tubes (Drummond Scientific Co.), and the tips were beveled to minimize damage to the oocytes during injection. The internal surface of each pipette was neutralized by dipping the unbeveled end in a siliconizing agent (Sigmacoate, Sigma Chemical Co.) and baking the pipettes, tips up, at 200°C for at least 1 h.

Electrophysiology and Experimental Protocol

Oocytes injected 3–6 d previously were perfused individually with an amphibian Ringer's solution containing 100.5 mM Na^+, 2 mM K^+, 1.8 mM Ca^{2+}, 1 mM Mg^{2+}, 105.6 mM Cl^-, and 5 mM HEPES (pH 7.5). Each oocyte was impaled with two microelectrodes, the membrane potential (V_m) was clamped using a two-electrode voltage clamp (TEV-200, Dagan Instruments, Minneapolis, MN), and membrane currents (I_m) were measured. The value of I_m at a holding potential of −60 mV was monitored continuously on a chart recorder. The membrane conductance (g) at −60 mV was determined by stepping V_m from −60 mV to −120 mV, then clamping V_m to voltages between −120 and +40 mV using a computer-driven ramp command (Clampex, Axon Instruments Inc., Foster City, CA) that changed the voltage at a rate of 100 mV/s. The I–V relationship was constructed from the digitized values of I_m and V_m, and the conductance at −60 mV was calculated from the slope of the I–V relationship between −70 and −50 mV.

The time course for activation of CFTR Cl^- conductance was determined by changing the oocyte perfusate to a Ringer's solution that contained 10 μM forskolin and 5 mM 3-isobutyl-1-methylxanthine (IBMX). Forskolin (Research Biochemicals International, Natick, MA or Sigma Chemical Co.) was added from a 20-mM stock in ethanol and IBMX (RBI or Sigma Chemical Co.) was added from a 500-mM stock in dimethylsulfoxide. In uninjected or water-injected oocytes, the membrane conductance at −60 mV was not affected by the cocktail of forskolin and IBMX, but in oocytes expressing CFTR, a time-dependent increase in membrane conductance was elicited (see Drumm et al., 1991). The maximum possible concentration of IBMX (5 mM) was chosen to maximize the activation rate of cAMP-dependent protein kinase and to optimize the activation level of insensitive CFTR

mutants so that all variants could be compared under identical conditions. The time course for activation was determined by measuring the conductance periodically until no further increase was discernible, indicating the establishment of an activated steady state. The CFTR Cl^- conductance activated at any time after addition of forskolin and IBMX, $g_{Cl}(t)$, was calculated by subtracting the background conductance measured before the addition of the drugs. To account for variability in the activation rates caused by differences in the level of CFTR expression among oocytes, the values of $g_{Cl}(t)$ were normalized to the maximum conductance, $g_{Cl}(max)$, measured in the activated steady state.

The activation of CFTR Cl^- conductance was described over most of its time course by a single exponential, as illustrated for wild type CFTR in Fig. 1. The activation rate was quantified by fitting a single exponential function to the data points between 15 and 85% of maximal activation. This range effectively excluded very early times, during which activation of the cytosolic enzymes was likely to be rate limiting, and very late times, when the rate of rise was slow and more difficult to quantify.

To examine the kinetics of CFTR deactivation, we monitored the time course for deactivation of CFTR Cl^- conductance after washout of forskolin and IBMX from the perfusate. Membrane conductance was measured in the activated steady state and periodically after changing the perfusate back to normal Ringer's solution, until no further change was discernible. The activated CFTR conductance remaining at any time after the solution change (time 0) was estimated by subtracting the value of the minimum membrane conductance measured in the deactivated steady state. These values were then normalized to the maximum value of g_{Cl} observed during the deactivation time course.

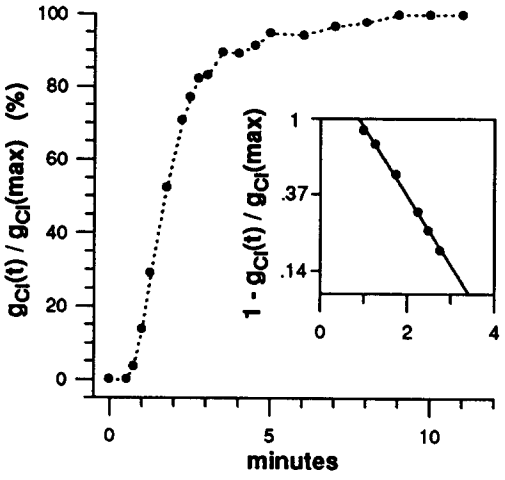

FIGURE 1. Representative time course for activation of wild-type CFTR expressed in *Xenopus* oocytes. CFTR Cl^- conductance (g_{Cl}) was determined periodically after addition (at time 0) of 10 μM forskolin and 5 mM IBMX to the oocyte perfusate. The measured values, $g_{Cl}(t)$, are plotted as a percentage of the maximum value, $g_{Cl}(max)$, measured in the activated steady state. In this experiment, the value of $g_{Cl}(max)$ was 23.4 μS and the background membrane conductance before stimulation was 1.9 μS. The inset shows the normalized conductance values between 15 and 85% of $g_{Cl}(max)$ plotted on a natural logarithmic scale, for estimation of $(k_{on} + k_{off})$ according to Eq. 1. From the linear regression (*solid line*), the value of $(k_{on} + k_{off})$ was 0.866 min^{-1} with a regression coefficient (r^2) of 0.992.

The deactivation of CFTR Cl^- conductance was more complex than activation, as illustrated in Fig. 2. Representative time courses are shown for wild type CFTR and two variants, K464Q and K1250Q. The former exhibits reduced steady state sensitivity to activation, whereas the latter exhibits increased sensitivity (Smit et al., 1993). The characteristic time course for deactivation of wild-type CFTR was a transient increase in g_{Cl} followed by a decline toward baseline. We interpreted the increase in g_{Cl} as the relief of IBMX block of CFTR, which has been documented in studies of single CFTR channels (Richards, Marth, and Dawson, unpublished observations; Schultz et al., 1994). The transient increase in g_{Cl} was most evident for wild-type CFTR and mutants such as K1250Q, which remained fully activated for several minutes after washout of IBMX. In contrast, the decline in g_{Cl} for mutants such as K464Q was rapid, showing only a slight increase after IBMX withdrawal. In view of this transient behavior, we chose to characterize the rate of deactivation in terms of two parameters: (*a*) the latency between drug removal (time 0) and deactivation to 85% of maximum g_{Cl}, and (*b*) the rate of decline between 85 and 15% of maximum g_{Cl}. For wild-type CFTR, the second component appeared to consist of two phases, an initial slow decline followed by a faster decline, but for comparison this was approximated by a single exponential decay because for all of the CFTR mutants examined here, the second component was well described by a single exponential (Fig. 2).

Interpretation of Activation and Deactivation Rates

In view of the fact that the rates of activation for wild-type and the mutant CFTRs examined here were dominated by single exponential time courses, we interpreted the rate of approach to the steady state g_{Cl} in terms of a model that recognizes only two states, inactive (I) and active (A).

$$I \underset{k_{off}}{\overset{k_{on}}{\rightleftharpoons}} A.$$

In this scheme, k_{on} represents the lumped rate coefficient for reactions and conformational changes that contribute to establishing the active state, and k_{off} represents the lumped rate coefficient for the reactions and conformational changes involved in the return to the inactive state. The coefficient k_{off} is a measure of the stability of the activated state under activating conditions and should be distinguished from the off rate that was measured following removal of the activating stimulus. We designate this latter parameter as $*k_{off}$, which is a measure of the stability of the active state in the absence of activating conditions (see below).

For the two-state model, the rate of approach of g_{Cl} to steady state activation is described by

$$g_{Cl}(t) = g_{Cl}(max) \cdot (1 - exp[-(k_{on} + k_{off})\, t]), \qquad (1)$$

and the value of $(k_{on} + k_{off})$ is given by the slope of a semilogarithmic plot of $1 - g_{Cl}(t)/g_{Cl}(\text{max})$ vs t. The values of k_{on} and k_{off} that characterize the approach to steady state activation can be calculated if the apparent $K_{1/2}$ for steady state activation (K_A) is known. The dose-dependent, steady state activation of CFTR by IBMX can be described by a single rectangular hyperbola. In previous studies (Drumm et al., 1991; Smit et al., 1993), we estimated the apparent K_A for dose-dependent activation from loga-

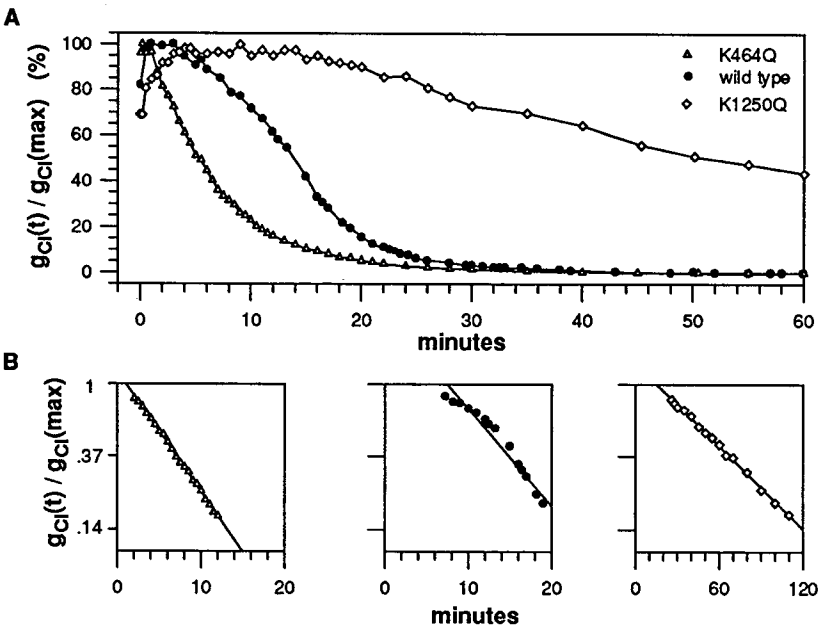

FIGURE 2. (*A*) Representative time courses for deactivation of wild type CFTR (●) and the analogous lysine to glutamine mutants in NBF1 (K464Q, △) and NBF2 (K1250Q, ◇). CFTR Cl^- conductance (g_{Cl}) was determined periodically after removal of forskolin and IBMX from the oocyte perfusate. The measured values, $g_{Cl}(t)$, are plotted as a percentage of the maximum value, $g_{Cl}(max)$, measured during deactivation. In the experiments shown, the values of $g_{Cl}(max)$ for wild-type CFTR, K464Q, and K1250Q were 27.9, 36.3, and 30.3 μS, and the corresponding minimum membrane conductances after deactivation of CFTR were 2.1, 0.7, and 1.0 μS, respectively. Deactivation time courses were characterized by two components: (*a*) a latency period, during which g_{Cl} increased transiently to $g_{Cl}(max)$ then decreased to 85% of $g_{Cl}(max)$, followed by (*b*) a further deactivation that was approximated by a single exponential. (*B*) Normalized conductance values between 85% and 15% of $g_{Cl}(max)$ are plotted on a natural logarithmic scale for estimations of $^*k_{off}$ according to Eq. 7. For *wild-type* (●), *K464Q* (△), and *K1250Q* (◇), the values of $^*k_{off}$ determined from linear regressions (*lines*) were 0.134, 0.166, and 0.019 min^{-1}, and the corresponding regression coefficients (r^2) were 0.957, 0.999, and 0.998, respectively.

rithmic dose–response plots, but for comparison with rates of activation we sought a more unbiased estimate of K_A that took into account three factors: (*1*) the activation produced by forskolin alone, (*2*) the block of CFTR by high concentrations of IBMX, and (*3*) the fact that for insensitive mutants such as G551D, D572N, and G1349D the dose–response showed no tendency toward saturation at the highest concentrations of IBMX. Accordingly, we assumed that if the steady state dose–response data were corrected for the small response in the presence of forskolin alone, then the activated g_{Cl} would be the sum of two components, one caused by activation of CFTR by IBMX and a second caused by blockade of activated CFTR by IBMX:

$$g_{Cl}/g_{Cl}^{max} = \left(g_{Cl}^{m}/g_{Cl}^{max}\right)\cdot [IBMX]/ ([IBMX] + K_A) - \left(g_{Cl}^{m}/g_{Cl}^{max}\right)\cdot [IBMX]/([IBMX] + K_I), \quad (2)$$

where g_{Cl}/g_{Cl}^{max} is the ratio of the steady state conductance activated by a particular concentration of IBMX to the maximum IBMX-activated conductance actually observed in the same experiment, g_{Cl}^{m} is the hypothetical maximum g_{Cl} that would be observed at maximum activation of CFTR in the absence of block, and K_A and K_I are the values of $K_{1/2}$ for activation and block, respectively. The block of CFTR by IBMX was assumed to represent a unimolecular binding event. Single-channel records suggest that the kinetics of block are fast, reducing the apparent amplitude of single-channel currents (Richards et al., unpublished observations; Schultz et al., 1994). We assumed that the maximum blockable conductance was equal to the maximum activatable conductance and that the value of K_I was the same for all of the CFTR variants examined.

The K_I for IBMX block was estimated from the response of the hypersensitive mutant, K1250A. Because K1250A is maximally activated at an IBMX concentration of ~1 mM, the block by higher concentrations of IBMX is readily apparent. The continuous curve in Fig. 3 *A* shows the fit of Eq. 2 to the dose–response data. Nonlinear regression yielded values of $g_{Cl}^{m}/g_{Cl}^{max} = 1.17 \pm 0.03$ and $K_I = 9.5 \pm 1.4$ mM. Values of K_A for wild type and all of the mutants were obtained by assuming that the value of K_I for IBMX block was 9.5 mM. Eq. 2 was fit to the data from individual experiments to provide the most unbiased estimate of the variance in K_A.

The value of g_{Cl}^{m}/g_{Cl}^{max} estimated for the mutant K1250A indicated that the maximum g_{Cl} actually observed, g_{Cl}^{max}, was nearly equal to the maximum possible activation, g_{Cl}^{m}, presumably because this conductance is achieved at an IBMX concentration of 1 mM, where block is minimal. The calculated curves for activation and block of K1250A are shown in Fig. 3 *A*, where the values of g_{Cl} are normalized to the theoretical maximum, g_{Cl}^{m}. For this mutant, the two components of the dose–response to IBMX are well separated such that at concentrations of IBMX below ~1 mM the activation of CFTR predominates, whereas at higher concentrations the conductance is progressively attenuated by IBMX block. The magnitude of the transient increase in g_{Cl} for K1250A after removal of 5 mM IBMX in the rate experiments (cf. Fig. 5 *B*) was consistent with this interpretation. The peak value of g_{Cl} measured during the deactivation time course was ~35% greater than the value measured in the presence of 5 mM IBMX, as predicted for a K_I of 9.5 mM.

For wild-type CFTR and the mutant K464Q, the observed values of g_{Cl}^{max} were ~60% and 27% of the theoretical maximum g_{Cl}, respectively. For these CFTR variants, the activated g_{Cl} does not approach the theoretical maximum conductance for two reasons: (*a*) the values of K_A are higher, so the activated g_{Cl} is proportionately lower at any concentration of IBMX, and (*b*) the

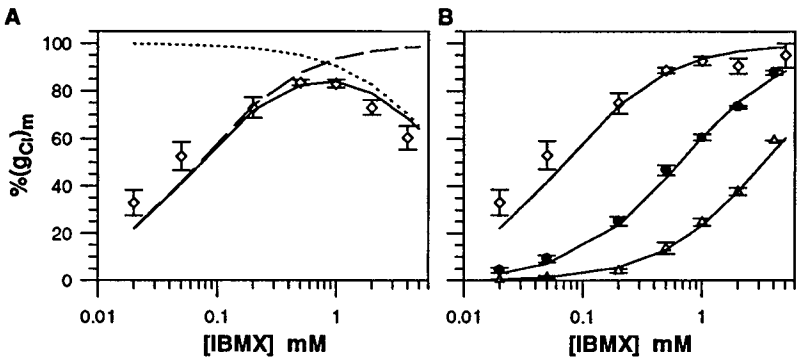

FIGURE 3. The IBMX dose–response relationships for steady state activation and block of CFTR. Values of g_{Cl} were measured in the presence of 10 μM forskolin alone and in combination with progressively increasing concentrations of IBMX. Dose–response relations were determined by subtracting the forskolin-stimulated g_{Cl} and normalizing the values of IBMX-stimulated g_{Cl} to the maximum value, g_{Cl}^{max}, measured in the same oocyte. The fit of Eq. 2 to the combined data for the hypersensitive mutant K1250A yielded a value of K_I for the block by IBMX, as described in the text. (*A*) The plotted points (◇) are means ± SEM for 10 oocytes expressing the mutant K1250A. The measured values of g_{Cl} are shown normalized to the theoretical maximum, g_{Cl}^{m}. The continuous curve shows the fit of Eq. 2, and the dashed and dotted curves show, respectively, the components of activation (K_A = 0.07 mM) and block (K_I = 9.5 mM). (*B*) IBMX dose–response relations for steady state activation of K1250A (◇), wild-type CFTR (●, n = 26), and K464Q (△, n = 5). The data points were corrected for block using K_I = 9.5 mM. The continuous curves show the activation predicted by the values of K_A, which were 0.07, 0.65, and 3.3 mM, respectively.

block by IBMX becomes appreciable above 1 mM. In Fig. 3 *B*, the activation components for wild-type CFTR and the mutants K1250A and K464Q were simulated by adding back the blocked component and plotting the adjusted data points along with the curves calculated using the estimated K_A values.

In view of the hyperbolic dose–response for steady state activation (Fig. 3 *B*) and the first-order kinetics of activation (Fig. 1), we assumed that the k_{on} for CFTR activation could be expressed as the product of the IBMX concentration and a lumped, pseudo first-order rate coefficient, k'_{on}, where

$$k_{on} = k'_{on}[\text{IBMX}] , \quad (3)$$

and the value of K_A for steady state activation is given by

$$K_A = k_{off}/k'_{on} . \quad (4)$$

Using these relations, values for k'_{on} and k_{off} in the activated steady state (5 mM IBMX) can be calculated from the measured values of $(k_{on} + k_{off})$:

$$k'_{on} = (k_{on} + k_{off})/([\text{IBMX}] + K_A) \quad (5)$$

and

$$k_{off} = (k_{on} + k_{off})/(1 + [\text{IBMX}]/K_A) . \quad (6)$$

As indicated previously, the rate of deactivation of g_{Cl} after abrupt removal of the activating conditions was complex and was described by two empirical parameters, a latency to 85% of $(g_{Cl})_{max}$ and an exponential decline given by

$$g_{Cl}(t) = g_{Cl}(\text{max}) \cdot \exp[-{}^{*}k_{off}t] , \quad (7)$$

where g_{Cl}(max) is the peak value of g_{Cl} during washout of IBMX and forskolin, and $^{*}k_{off}$ is the exponential off rate following the initial transient in $g_{Cl}(t)$. The values of $^{*}k_{off}$ tended to be greater than the corresponding estimates of k_{off}, the calculated off rate under activating conditions, as expected if some feature of these conditions reduced the deactivation rate. For example, IBMX may inhibit phosphatase activity, as suggested by the work of Becq et al. (1993), and/or IBMX itself may stabilize the active state of CFTR (Schultz et al., 1994). Generally, however, mutations induced qualitatively similar changes in k_{off} and $^{*}k_{off}$, suggesting that these two independent measures provide similar impressions of changes in the stability of the active state of CFTR.

Statistical Comparisons

The values of K_A and the rate analysis parameters for each mutant were compared with those for wild-type CFTR and with those for other mutants using a one-way analysis of variance and Fisher's post hoc test of least significant differences. Analysis of variance is most appropriate if the variance is constant across individual groups, but in the present case the variance tended to be proportional to the magnitude of the parameter in question. Therefore, the variance for each parameter was stabilized before statistical analysis by taking the logarithm of all values (Snedecor and Cochran, 1967).

RESULTS

Mutations in the Nucleotide Binding Folds Dramatically Altered the Rates of Activation and Deactivation of CFTR

The rate of activation of CFTR in oocytes is determined by the properties of a multistep reaction, which involves not only the dynamics of CFTR itself but also the properties of cellular enzyme systems governing the activities of protein kinases and phosphatases. To minimize the time required for elevation of cytosolic cAMP and protein kinase A activity, we used forskolin and the maximum possible concentration of the phosphodiesterase inhibitor, IBMX. Mutations in CFTR can be reasonably expected to affect the response of CFTR to activating conditions, but not the dynamics of cellular enzyme systems. In the course of this study, we found that NBF mutations associated with altered values for the $(K_A)_{IBMX}$ caused dramatic changes in the macroscopic kinetic parameters measured here. The values listed in Table I show that NBF mutations generally reduced the value of $(k_{on} + k_{off})$, in some cases by more

TABLE I

Summary of Activation and Deactivation Data for Wild-type CFTR and Mutants of the Invariant Glycine in NBF1 (G551) or NBF2 (G1349)

			Activation					Deactivation		
CFTR	K_A (mM)	n	$(k_{on} + k_{off})$ (10^{-3} min^{-1})	k'_{on} (10^{-3} min^{-1} mM^{-1})	k_{on} (10^{-3} min^{-1})	k_{off} (10^{-3} min^{-1})	n	latency (min)	$*k_{off}$ (10^{-3} min^{-1})	n
wt	0.65 ± 0.08	26	664 ± 51	118 ± 9	588 ± 45	76 ± 6	20	6.0 ± 0.3	88 ± 6	16
G551A	3.0 ± 0.5*‡	6	104 ± 5*‡	13 ± 0.6*‡	65 ± 3*‡	39 ± 2*	5	7.7 ± 0.5‡	70 ± 13‡	4
G551S	4.7 ± 0.5*	5	82 ± 6*‡	8 ± 0.6*‡	42 ± 3*‡	40 ± 3*‡	10	3.9 ± 0.3*‡	88 ± 6‡	6
G551D	9.3 ± 0.01*	6	57 ± 9*‡	4 ± 0.6*‡	20 ± 3*‡	37 ± 6*‡	5	1.8 ± 0.2*‡	84 ± 10‡	6
G1349A	1.1 ± 0.07*‡	5	210 ± 24*‡	35 ± 4*‡	172 ± 20*‡	38 ± 4*	4	1.7 ± 0.3*‡	184 ± 20*‡	5
G1349S	3.5 ± 0.3*	4	199 ± 46*‡	23 ± 5*‡	117 ± 27*‡	82 ± 19‡	6	2.3 ± 0.5*‡	144 ± 15*‡	6
G1349D	9.3 ± 0.01*	8	114 ± 16*‡	8 ± 1*‡	40 ± 6*‡	74 ± 11‡	5	0.6 ± 0.1*‡	286 ± 37*‡	4

Values were determined as described in Methods. The symbols (*) and (‡) indicate significant differences from wild-type CFTR and the analogous mutant, respectively ($P < 0.05$).

than 10-fold. Likewise, values for the latency and $*k_{off}$ were markedly mutant dependent, the former decreasing by as much as 10-fold or increasing by as much as 3.7-fold compared with the wild type. Such changes are consistent with the notion that the rates of activation and deactivation measured here reflect the kinetics of the conversion of CFTR from an inactive to an active state. Using the values of K_A and $(k_{on} + k_{off})$ listed in Table I, it is possible to calculate values for the apparent k_{on} (or k'_{on}) and k_{off} that characterize the approach to steady state activation. For wild-type CFTR, for example, $k_{on} = 0.588 \pm 0.045$ min^{-1} ($k'_{on} = 0.118 \pm 0.009$ min^{-1} mM^{-1}) and $k_{off} = 0.076 \pm 0.006$ min^{-1}, suggesting that, at 5 mM IBMX, the rate of relaxation was dominated by the on rate, as expected. A strict interpretation of these rates in terms of a two-state, closed–open channel-gating process would require closed times of the order of 1.7 min and open times of ~13 min. The gating of CFTR Cl^- channels in cell-attached membrane patches has not been studied extensively, but there is no suggestion in the available data for open and closed times of this magnitude. This suggests that there is a slow component to the dynamics of CFTR activation that is reflected in the rates determined here (see Discussion). In addition, however, it is possible that the activation rate may be artifactually reduced by the finite rate of rise of intracellular PKA activity. Despite this possible attenuation, the relative changes in kinetic parameters associated with NBF mutations provide an approach to characterizing the mutation-induced changes in accessibility or stability of the active state.

Our mutational analysis focused on three residues that can be identified unambiguously in the two NBFs because of their locations within primary sequence motifs either in ATPases generally or specifically within the family of traffic ATPases. In each NBF, we substituted the invariant glycine (G551 in NBF1 or G1349 in NBF2), which lies in a region that is characteristic of traffic ATPases (Hyde et al., 1990; Mimura et al., 1991), is invariant among CFTRs of different species (Diamond et al., 1991; Tucker et al., 1992), and is associated with mutations that cause cystic fibrosis (Cutting et al., 1990; Kerem et al., 1990; Strong et al., 1991). The other two sites lie within primary sequence motifs that form part of the nucleotide binding pocket in ATPases and GTPases for which crystal structures are available (see Discussion). The Walker consensus A motif (Walker et al., 1982) forms a glycine-rich, phosphate-binding loop in the hydrolytic core of ATPases and GTPases, and the invariant lysine near the carboxyl end of this motif participates in the binding and hydrolysis of ATP through associations with the β- and γ-phosphates of ATP. The Walker consensus B motif (Walker et al., 1982) is also located within the phosphate-binding portion of the binding pocket, and the highly conserved aspartic acid at the carboxyl end of this motif may also participate in ATP hydrolysis. In Results and Discussion, we refer to the invariant glycine in relation to G551 in NBF1 or G1349 in NBF2 and to the ATP-binding pocket in reference to the Walker consensus A lysines (K464 in NBF1 and K1250 in NBF2) or the consensus B aspartic acids (D572 in NBF1 and D1370 in NBF2). Although there is presently no definitive structural information for either NBF of CFTR, this nomenclature is useful for presenting the results of mutations at these sites.

Steady State Activation of NBF Mutant CFTRs

The values of K_A obtained by curve fitting (Table I) are in accord with the qualitative analysis presented previously (Smit et al., 1993). The values of K_A determined for the mutant CFTRs all differed significantly from that of wild-type CFTR ($P < 0.05$). Substitutions for the invariant glycine in either NBF produced similar increases in K_A, with the exception of the mutation that

was conservative with respect to polarity and size, alanine for glycine, which in NBF1 (G551A) produced a nearly fivefold increase in K_A but in NBF2 (G1349A) produced less than a twofold increase. In contrast, substitutions for conserved residues in the putative ATP binding pocket produced opposing effects on K_A. Substitutions in NBF1 increased K_A from fourfold to 14-fold over that seen with wild-type CFTR, whereas the comparable substitutions in NBF2 decreased K_A by fourfold to ninefold. These differential shifts in K_A were an initial indication that NBF1 and NBF2 play different roles in the activation of CFTR.

Rate Analysis of Invariant Glycine Mutants

Substitutions for the invariant glycine in either NBF1 (G551) or NBF2 (G1349) significantly slowed the rate of approach to steady state activation ($k_{on} + k_{off}$) compared with wild-type CFTR, and the reductions produced by the substitutions in NBF1 were more profound than those produced by the analogous substitutions in NBF2 ($P < 0.05$). The reductions in the relaxation rates can be seen clearly in the representative traces shown in Fig. 4 *A* and in the values of ($k_{on} + k_{off}$) listed in Table I. In NBF1, substitution to alanine (G551A), the most conservative change possible, reduced the relaxation rate by more than sixfold, and the less conservative substitutions to serine (G551S) and aspartic acid (G551D) progressively reduced the relaxation rate. At the analogous site in NBF2, the most conservative substitution (G1349A) also reduced the relaxation rate, but by only about threefold. Substitutions to serine (G1349S) and aspartic acid (G1349D) produced progressive reductions such that the relaxation rate for the least conservative mutation, G1349D, was about twice that for the comparable mutation in NBF1.

The values of ($k_{on} + k_{off}$) observed with the analogous mutations in NBF1 and NBF2 suggested that the observed increases in K_A (k_{off}/k'_{on}) arose primarily from a decrease in the on rate. This impression is confirmed by an examination of the values calculated for the apparent k'_{on} and k_{off}, which are shown in Table I and compared in Fig. 5. Substitutions for G551 in NBF1 reduced the on rate more dramatically than the analogous substitutions for G1349 in NBF2. In NBF1, these substitutions reduced the on rate by 9- to 30-fold and slightly reduced the apparent off rate under activating conditions (k_{off}), suggesting that the increase in K_A was due to a reduction in the accessibility of the active state

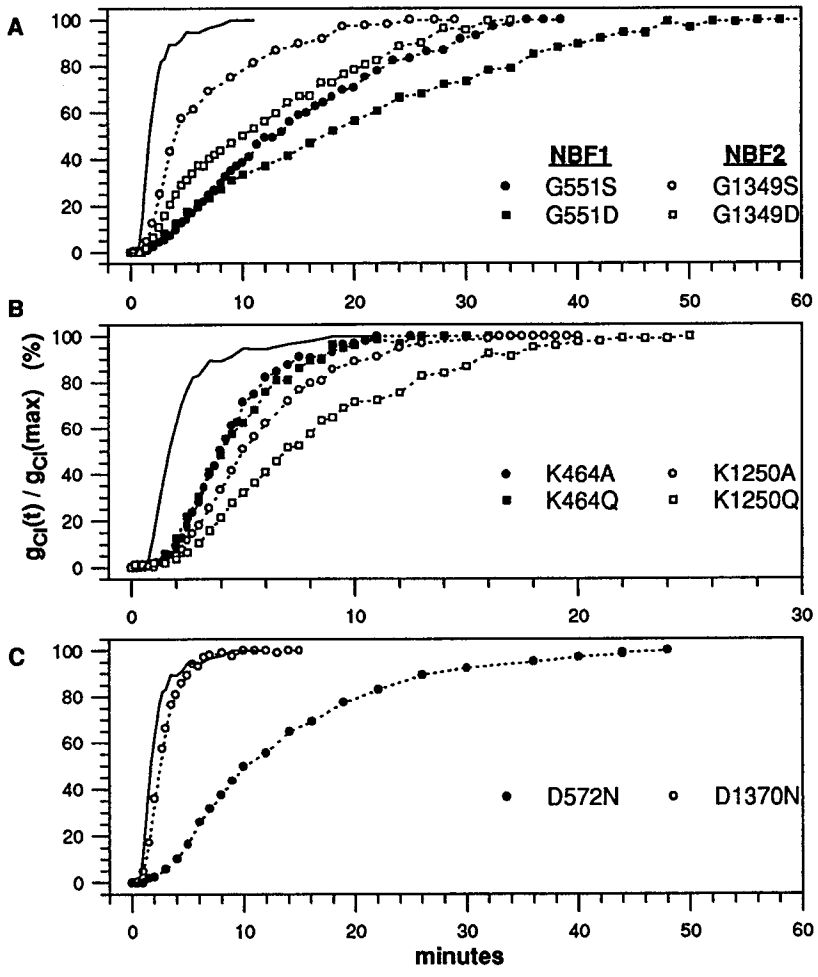

FIGURE 4. Representative time courses for activation of CFTR mutants with substitutions of analogous amino acids in NBF1 (*solid symbols*) and NBF2 (*open symbols*). Analogous mutations are designated within each panel by symbols of the same shape. The representative time course for wild-type CFTR (Fig. 1) is replotted in each panel for reference (*solid line*). (*A*) Substitutions of the invariant glycine in *NBF1* (*G551*) or *NBF2* (*G1349*) by serine (*S*, ●, ○) or aspartic acid (*D*, ■, □). (*B*) Substitutions of the Walker consensus A lysine in the ATP binding pocket of *NBF1* (*K464*) or *NBF2* (*K1250*) by alanine (*A*, ●, ○) or glutamine (*Q*, ■, □). Note the different time scale. (*C*) Substitutions of asparagine for the Walker consensus B aspartic acid in the ATP-binding pocket of *NBF1* (*D572N*, ●) or *NBF2* (*D1370N*, ○).

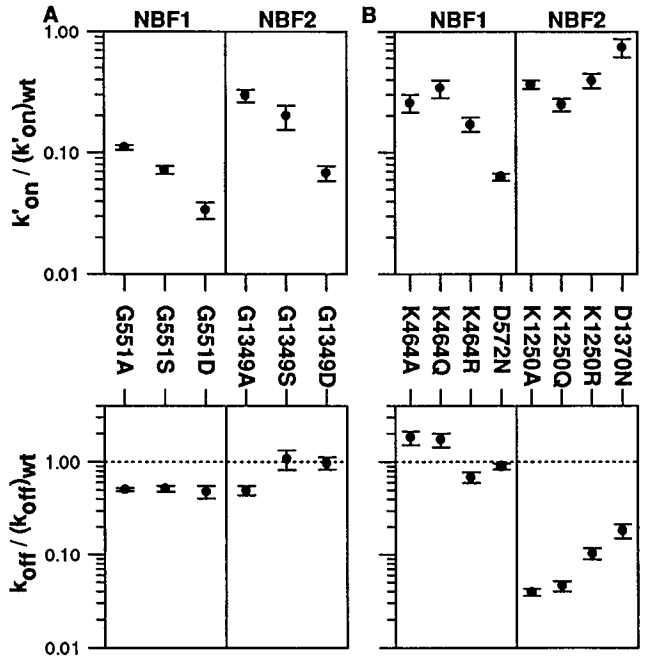

FIGURE 5. Summary of mutation-induced effects on the activation parameters. Values for the pseudo–first-order on-rate coefficient (k'_{on}) and for the off-rate coefficient (k_{off}) were calculated using the measured values of (k_{on} + k_{off}) and the corresponding estimates of K_A (Eqs. 5 and 6). Points are means ± SEM for the ratios of the mutant values to the mean wild-type value (number of experiments listed in Table I or Table II). (*A*) Mutants of the invariant glycine in *NBF1* (*G551*) or *NBF2* (*G1349*). (*B*) Mutants of the Walker consensus A lysine or consensus B aspartate in the ATP-binding pocket of *NBF1* (*K464, D572*) or *NBF2* (*K1250, D1370*).

that was ameliorated slightly by a smaller but significant stabilization of this state. The analogous substitutions in NBF2 also reduced the on rate, but only by 3- to 15-fold. Here also, the increase in K_A was primarily due to reduced accessibility of the active state. In either NBF, the progressively less conservative substitutions to alanine, serine, and aspartic acid induced significantly greater attenuations of the on rate.

Comparisons of the deactivation rates for glycine-substituted mutants (Table I) revealed differential effects on the stability of the active state that were not apparent in the calculated values of k_{off}. Representative time courses for deactivation of NBF1 and NBF2 mutants are shown in Fig. 6 *A*, and values for the latency and $*k_{off}$ are compared in Fig. 7 *A*. Substitutions for the invariant glycine in NBF2 (G1349) severely compromised the stability of the active state. Here, even the most conservative replacement (G1349A) dramatically shortened the latency and significantly increased the rate of exponential decline. This destabilization of the activated state is clearly evident in the representative time courses for deactivation of the mutants G1349S and G1349D (Fig. 5 *A*).

The effects of substitutions for the invariant glycine in NBF1 (G551) on deactivation were generally less substantial. The most conservative substitution (G551A) did not appreciably alter the latency. The less conservative substitutions (G551S, G551D) progressively decreased the latency, but the reductions were always less than those induced by the corresponding mutations (G1349S, G1349D) in NBF2. The progressive destabilization of the active state suggested by the decreased latency seen with the G551S and G551D substitutions was not evident, however, in the subsequent phase of exponential decline. The values of $*k_{off}$ were similar to that for wild-type CFTR.

Rate Analysis of ATP-Binding Pocket Mutants

The rates of approach to steady state activation for mutants of the putative ATP-binding pockets confirmed the impression that both NBF1 and NBF2 are involved in gaining access to the active state and suggested that NBF2 is particularly important for determining the stability of the active state. The representative time courses in Fig. 4 *B* show that substitutions for the Walker consensus A lysine in either NBF produced comparable reductions in the relaxation rate (k_{on} + k_{off}). As shown in Table II, substitutions for the lysine in NBF1 (K464) reduced the relaxation rate (k_{on} + k_{off}) and increased K_A (k_{off}/k'_{on}), so the decrease in the relaxation rate was due to a decrease in the on rate. The effects of the alanine, glutamine, and arginine substitutions were similar, resulting in 66–83% decreases in k'_{on}. Although significant, these reductions were somewhat less than those seen with the substitutions for the invariant glycine in NBF1 (G551). The calculated values of k_{off} for K464Q and K464A indicated that the substitutions to alanine or glutamine also increased the off rate under activating conditions, which contributed to the increase in K_A and compensated somewhat for the reduction in relaxation rate caused by the reduced on rate. In contrast, the more conservative arginine substitution actually appeared to cause a modest stabilization of the active state.

The comparable substitutions for the lysine in NBF2 (K1250) produced relaxation rates that were generally similar to those seen with their NBF1 counterparts, because of similar reductions in the on rate (k'_{on}). In addition, however, substitutions at this site produced a profound reduction in the apparent k_{off}. Although this additional reduction in the off rate was not immediately apparent in the relaxation rates (k_{on} + k_{off}) because of the proportionately small contribution of the off rate, this apparent stabilization of the active state accounts for the values of K_A that were from 3.8- to 9-fold smaller than that for wild-type CFTR, rendering these mutants hypersensitive to activating conditions.

The substitution of asparagine for the Walker con-

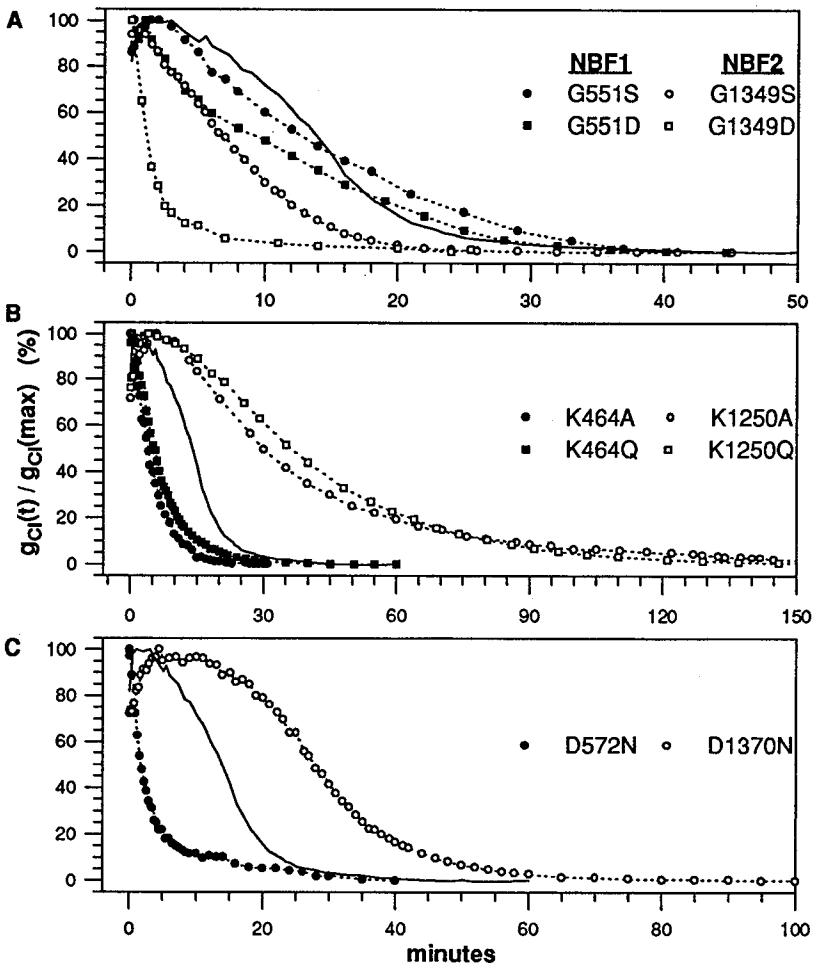

FIGURE 6. Representative time courses for deactivation of CFTR mutants with substitutions of analogous amino acids in NBF1 (*solid symbols*) and NBF2 (*open symbols*). Designations are the same as those in Fig. 4. The representative time course for wild-type CFTR (Fig. 2) is replotted in each panel for reference (*solid line*). Note the different time scales. (*A*) Mutants of the invariant glycines. (*B*) Mutants of the Walker consensus A lysines. (*C*) Mutants of the Walker consensus B aspartic acids.

sensus B aspartic acid in NBF1 (D572N) produced a profound reduction in the rate of approach to steady state activation (Fig. 4 *C*); the value of (k_{on} + k_{off}) was comparable with that seen with the G551A mutation (cf. Tables I and II). Although the calculated parameters are less reliable because of the relatively high value of the apparent K_A, the value of the apparent k'_{on} is consistent with a marked reduction in the accessibility of the active state whereas the apparent off rate was not different from that of wild-type CFTR. In contrast, the analogous substitution in NBF2 (D1370N) produced only a modest decrease in (k_{on} + k_{off}), evident in Fig. 4 *C*. The values of the derived parameters (k'_{on}, k_{off}) for this slightly hypersensitive mutant, however, suggest that the decrease in K_A was a reflection of a fourfold decrease in k_{off}, whereas the apparent k'_{on} was not significantly different from that of wild-type CFTR.

Values of the calculated k_{off} for CFTRs bearing mutations in the putative nucleotide binding pocket of NBF1 or NBF2 suggested that these two domains play different roles as regards the stability of the active state. This dichotomy was also evident in the deactivation parameters that were measured directly (Fig. 5, *B* and *C*). In NBF1, substitutions for the consensus A lysine (K464) or the consensus B aspartic acid (D572) decreased the latency to 15–32% of the value for wild-type CFTR and significantly increased the measured off rate ($*k_{off}$), indicating destabilization of the active state (Table II, Fig. 7). In contrast, substitutions at the analogous sites in NBF2 (K1250 or D1370) actually increased the latency by two- to threefold, and, with the exception of the most conservative substitution, K1250R, the values of $*k_{off}$ were decreased compared with that of wild-type CFTR, indicating stabilization of the active state. These results suggest that the consensus A lysine and consensus B aspartic acid in the ATP binding pocket of NBF1 contribute to stabilization of the active state, whereas their analogues in NBF2 are involved in terminating the active state. Particularly noteworthy in this regard is the D1370N mutation, which produced no significant effect on the apparent on rate but markedly delayed deactivation.

In NBF2, the effects of substitutions at sites in the putative ATP-binding pocket (K1250 and D1370) on deactivation were clearly opposite to the effects of substitutions for the invariant glycine (G1349). The former markedly delayed deactivation, as reflected in the increased latency and decreased $*k_{off}$, whereas the latter

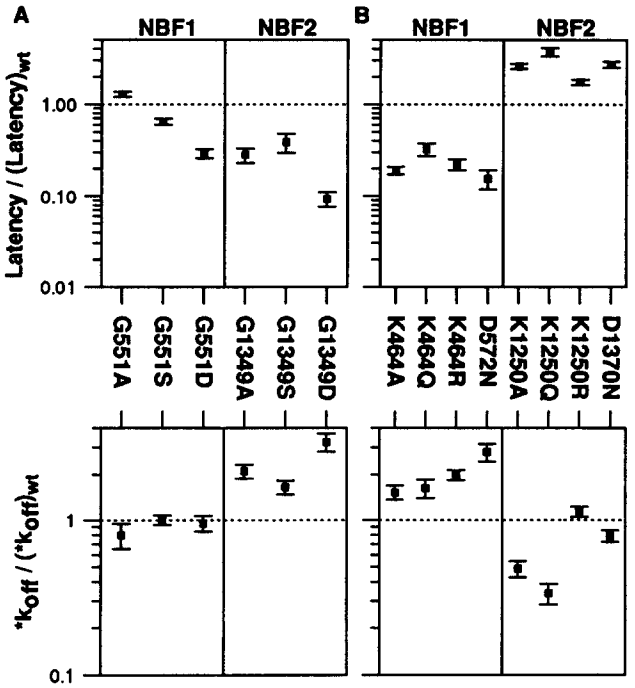

FIGURE 7. Summary of mutation-induced effects on the deactivation parameters. The latency is the time elapsed between removal of the activating stimulus (time 0) and deactivation of g_{Cl} to 85% of g_{Cl}(max), and $*k_{off}$ is the measured rate coefficient for the subsequent exponential phase of deactivation. Plotted values are the means ± SEM for the ratios of the mutant values to the mean wild-type value (number of experiments listed in Table I or Table II). *A* and *B* are the same as Fig. 6.

markedly hastened deactivation, as signaled by the reduced latency and increased $*k_{off}$ (cf. Figs. 5 and 7). In NBF1, mutations at sites in the ATP binding pocket (K464 and D572) also produced effects that were different from those of substitutions for the invariant glycine (G551). Here, however, mutations in the binding pocket clearly hastened deactivation, evidenced by decreases in the latency and increases in $*k_{off}$, while the mutations of glycine 551 moderately decreased $*k_{off}$. The latency was also decreased progressively by the less conservative mutations, G551S and G551D.

In general, the effects of mutations on the latency were mirrored by those on the value of $*k_{off}$, although the latter were often less marked. For example, the NBF2 glycine mutants exhibited increased values of $*k_{off}$ in conjunction with the decreased latency, as did the mutants of the NBF1 binding pocket. Similarly, the value of $*k_{off}$ was reduced for most of the NBF2 binding pocket mutants, which also exhibited increased latencies. There were exceptions to this pattern, however. For mutants of the NBF1 glycine (G551S and G551D), the values of $*k_{off}$ did not increase in conjunction with the progressively decreased latency. Similarly, although the K1250R and D1370N mutants exhibited an increased latency, the values of $*k_{off}$ were not significantly different from that of wild type CFTR.

DISCUSSION

Analyzing the functional properties of CFTRs bearing mutations in the nucleotide binding domains is one approach to testing hypotheses for the roles of these domains in activation and deactivation. Our analysis focused on analogous residues in two regions of each NBF: an invariant glycine (G551 or G1349) that is a signal feature of the traffic ATPase superfamily and two other residues, the invariant Walker A lysine (K464 or K1250) and the highly conserved Walker B aspartic acid (D572 or D1370), which are likely to lie within the hydrolytic core of the ATP-binding pocket. The results indicate that NBF1 and NBF2 play distinctly different,

TABLE II

Summary of Activation and Deactivation of Wild-type CFTR and Mutants of the Walker Consensus A Lysine or Consensus B Aspartic Acid in the ATP Binding Pocket of NBF1 (K464, D572) or NBF2 (K1250, D1370)

			Activation					Deactivation		
CFTR	K_A (mM)	*n*	$(k_{on} + k_{off})$ $(10^{-3}\ min^{-1})$	k'_{on} $(10^{-3}\ min^{-1}\ mM^{-1})$	k_{on} $(10^{-3}\ min^{-1})$	k_{off} $(10^{-3}\ min^{-1})$	*n*	latency (min)	$*k_{off}$ $(10^{-3}\ min^{-1})$	*n*
wt	0.65 ± 0.08	26	664 ± 51	118 ± 9	558 ± 45	76 ± 6	20	6.0 ± 0.3	88 ± 6	16
K464R	2.6 ± 0.1*‡	4	153 ± 20*‡	20 ± 3*‡	101 ± 13*‡	52 ± 7*‡	5	1.3 ± 0.2*‡	174 ± 14*‡	7
K464Q	3.3 ± 0.5*‡	5	331 ± 56*‡	40 ± 7*	199 ± 34*	132 ± 22*‡	5	1.9 ± 0.3*‡	142 ± 19*‡	5
K464A	4.6 ± 0.7*‡	6	289 ± 49*	30 ± 5*‡	151 ± 26*‡	139 ± 24*‡	7	1.1 ± 0.1*‡	133 ± 14*‡	8
D572N	9.3 ± 0.02*‡	6	106 ± 7*‡	7 ± 0.5*‡	37 ± 3*‡	69 ± 5‡	4	0.9 ± 0.2*‡	245 ± 32*‡	3
K1250R	0.17 ± 0.07*‡	5	239 ± 33*‡	46 ± 6*‡	231 ± 32*‡	8 ± 1*‡	10	10.4 ± 0.8*‡	100 ± 7‡	6
K1250Q	0.12 ± 0.04*‡	5	150 ± 18*‡	29 ± 4*	146 ± 18*	4 ± 0.4*‡	5	22.3 ± 2.4*‡	30 ± 5*‡	5
K1250A	0.07 ± 0.02*‡	10	218 ± 18*	43 ± 4*‡	215 ± 18*‡	3 ± 0.3*‡	5	15.6 ± 1.0*‡	43 ± 5*‡	5
D1370N	0.16 ± 0.04*‡	7	449 ± 79*‡	87 ± 15‡	435 ± 76‡	14 ± 2*‡	5	16.3 ± 1.2*‡	69 ± 6‡	5

The symbols (*) and (‡) indicate significant differences from wild-type CFTR and the analogous mutant, respectively ($P < 0.05$).

although overlapping, roles in the cycle of CFTR activation and deactivation. Both NBF1 and NBF2 are important for accessing the activated state, but the results of rate analysis suggest a dominant role for NBF1 in this process. Similarly, both NBFs influence the stability of the active state, but in different ways. Mutations in the ATP-binding pocket of NBF1 destabilized the active state, whereas the analogous mutations in NBF2 stabilized the active state, suggesting that NBF2 plays a major role in regulating the termination of the active state. The effects of mutations in the ATP binding pockets speak in favor of a role for ATP hydrolysis in the activities of both NBFs but suggest that at NBF1, ATP hydrolysis is associated with activating CFTR, whereas at NBF2, ATP hydrolysis provides a mechanism for timing the duration of the active state. Finally, the results suggest that within each NBF, the functional role of the invariant glycine (G551 or G1349) is distinctly different from those of either the lysine (K464 or K1250) or the aspartic acid (D572 or D1370) in the ATP-binding pocket.

NBF1: Activation and Stabilization

The results of rate analysis suggest that ATP-dependent processes involving NBF1 are critical for activating CFTR Cl^- channels and for maintaining the channels in the active state. This conclusion is based on the observation that substitutions in NBF1 profoundly affected both the accessibility and the stability of the active state. Substitutions for the invariant glycine (G551), the consensus A lysine (K464), or the consensus B aspartic acid (D572) reduced the value of k'_{on} (Fig. 6). In addition, the effects on the latency parameter suggest that the substitutions in either the consensus A or B regions of NBF1 markedly destabilized the active state. These findings are consistent with a scheme in which ATP hydrolysis at NBF1 is the crucial event in ATP-dependent activation and the active state is stabilized by some product of ATP hydrolysis.

A role for ATP hydrolysis at NBF1 in the activation of CFTR is supported by functional evidence from other laboratories. Using detached membrane patches from transfected NIH-3T3 fibroblasts, Anderson et al. (1991*a*) showed that after exposure to a phosphorylating environment, CFTR Cl^- channels were activated only in the presence of hydrolyzable ATP analogues, an observation subsequently confirmed in detached patches from transfected HeLa cells (Carson and Welsh, 1993), in guinea pig cardiac myocytes (Hwang et al., 1994), in lipid bilayers after fusion of membrane vesicles from transfected HEK 293 cells (Gunderson and Kopito, 1994), and in detached patches from transfected mouse L cells (Schultz et al., 1995). Phosphate analogues such as orthovanadate and beryllium trifluoride prolonged the opening of CFTR Cl^- channels, but only after they had been opened by ATP (Baukrowitz et al., 1994; Gunderson and Kopito, 1994). These effects were not definitively localized to NBF1 but are consistent with the notions that ATP hydrolysis is required for activation and that phosphate analogues stabilize the active state of CFTR by slowing the dissociation rate of the hydrolysis product, ADP. Thus, mutations in NBF1 that compromise either ATP binding or hydrolysis, or the coupling of these events to the channel-gating mechanism, would be predicted to slow activation, as seen with all of the NBF1 mutations examined here. Furthermore, mutations that reduce the affinity for the hydrolysis product ADP would be predicted to destabilize the active state, as seen here with mutations of the consensus A lysine or the consensus B aspartic acid in NBF1.

NBF2: Activation and Termination

A striking result of the mutational analysis was the finding that substitutions for the consensus A lysine (K1250) or the consensus B aspartic acid (D1370) in the putative ATP-binding pocket of NBF2 dramatically stabilized the active state of CFTR. These findings suggest that an interaction of ATP at NBF2 regulates the duration of the active state. This notion is consistent with the observations of Hwang et al. (1994), who showed that the nonhydrolyzable ATP analogue, AMP-PNP, could stabilize the open state of cardiac CFTR Cl^- channels previously opened by exposure to ATP. The interdependence of the actions of ATP and AMP-PNP was interpreted as an indication that after the binding or hydrolysis of ATP at one NBF (NBD_A), AMP-PNP could bind at a second site (NBD_B). The stabilizing effect of AMP-PNP on CFTR gating, also demonstrated by Gunderson and Kopito (1994), was interpreted as an indication that the rate of ATP hydrolysis at NBD_B times the duration of the active state. As discussed below, structural and functional studies of other ATPase proteins support the idea that substitutions for the consensus A lysine or the consensus B aspartate in the ATP-binding pocket would be likely to alter the rate of ATP hydrolysis. The rate analysis of CFTR mutants presented here is consistent with the notion that the NBD_B of Hwang et al. (1994) is, in fact, NBF2 and that ATP-dependent processes at this site regulate the termination of the active state. In a recent report, Gunderson and Kopito (1995) presented evidence for a cyclic gating scheme for CFTR comprising at least one closed and two distinct open states, O_1 and O_2, that were distinguished by a small difference in single-channel conductance. They proposed that ATP hydrolysis at NBF2 can regulate the stability of the open state of CFTR by controlling the transition from the more stable O_1 state to the less stable O_2 state.

The results from different laboratories regarding the

effects of the nonhydrolyzable analogue AMP-PNP on ATP-dependent gating of CFTR are not entirely consistent. Carson et al. (1995) studied CFTR gating in detached patches from stably transfected C127 mouse mammary cells. Exposure of wild-type CFTR to AMP-PNP prompted the appearance of a distinct population of longer openings, but these made a relatively small contribution to the open probability. Furthermore, in detached patches from mouse L cells, Schultz et al. (1995) found no effect of AMP-PNP on either open probability or the efficacy of ATP. The discrepancies between these results and those reported by Hwang et al. (1994) and Gunderson and Kopito (1994) could be related to the phosphorylation state achieved in detached patches or to other, as yet unresolved, methodologic differences. Schultz et al. (1995) called attention to a possible role for temperature in determining the gating kinetics of CFTR. Reducing the temperature from 35 to 25°C increased the open probability in multichannel patches to near unity, and this effect was observed only in the presence of PKA, despite the fact that the enzyme was not required to maintain activity with a lower open probability. Those results suggested that temperature, in addition to the phosphorylation state, is important for determining the gating state of CFTR. The present experiments were conducted at temperatures ranging between 19 and 21°C, and indicate clearly that in the intact oocyte maximally stimulated by forskolin and IBMX, mutations in NBF2 of CFTR can lead to a profound stabilization of the active state. Thus, in the oocyte, although CFTR gating may be slowed, it seems unlikely that this temperature, per se, increases P_o to near unity.

Structural alterations in NBF2 also significantly slowed the activation of CFTR. Thus, although the mutation analysis assigns to NBF2 a primary role in timing the active state, this domain is also clearly involved in accessing the active state. There are at least two ways in which NBF2 could function in the activation of CFTR. ATP-dependent events at NBF2 could contribute to the conformational changes that underlie channel opening in a manner that is independent of NBF1, or NBF2 could act by modulating or otherwise contributing to events at NBF1. The latter view was proposed by Baukrowitz et al. (1994) as a mechanism for the stabilizing effect of NBF2. Of particular interest in this regard was the effect of the NBF2 mutation, D1370N. This substitution increased the stability of the active state but failed to significantly alter the on rate. This dichotomy suggests that it is possible to interfere with the timing function of NBF2 without affecting its role in accessing the active state. If it is assumed that this substitution acts by reducing the rate of ATP hydrolysis but not ATP binding, then the results imply that the binding of ATP at NBF2 is sufficient for its participation in activation. In this view, ATP hydrolysis at NBF1 drives the conformation change that activates the channel, and NBF2 participates in activation as a modulator of events at NBF1.

Roles of the Consensus A Lysine and Consensus B Aspartic Acid

Structural studies of ATPase proteins offer some insights into the possible functional roles of the A and B consensus regions in NBF1 and NBF2 of CFTR. These regions form portions of the ATP-binding pockets in ATPase proteins with otherwise diverse primary sequences and functions. The consensus A motif, which forms a phosphate-binding loop (P-loop) common to both ATPase and GTPase proteins (Saraste et al., 1990), is identified by the amino acid sequence **G**-X-X-G-X-**G**-**K**-T/S, in which the bold glycines (G) and lysine (K) are invariant (Walker et al., 1982; Fry et al., 1986; Hyde et al., 1990; Mimura et al., 1991). The crystal structures of several ATPases and GTPases, including the F_1-ATPase (Abrahams et al., 1994), adenylate kinase (Müller and Schulz, 1992), the recA protein (Story and Steitz, 1992), and the G-protein $Gi\alpha_1$ (Coleman et al., 1994), indicate that this glycine-rich loop spans the hydrolytic core of the binding pocket and that the invariant lysine interacts directly with the β- and γ-phosphate groups of bound ATP, implying roles for this lysine in both the binding and hydrolysis of ATP. Mutations of this lysine to arginine in the yeast RAD3 protein (Sung et al., 1988), to alanine in the *Escherichia coli* UvrA protein (Thiagalingam and Grossman, 1991), or to glutamine in the *E. coli* F_1-ATPase (Senior et al., 1993) impaired ATPase activity. ATP binding was not affected by the alanine substitution but was reduced by the arginine and glutamine substitutions, although these reductions were less marked than the reductions in ATPase activity.

The common location and apparently conserved role of the Walker consensus A lysine among ATPases and GTPases with diverse structures and functions suggest strongly that the analogous lysines in CFTR are also located within the phosphate-binding, hydrolytic cores of the ATP-binding pockets in NBF1 and NBF2. Hence, substitutions for the lysine in NBF1 (K464) or NBF2 (K1250) of CFTR would be expected to impair both the binding and subsequent hydrolysis of ATP by the NBF bearing the mutation. The affinity for ADP is likely to be reduced also, as the analogous lysines in the recA and *ras* proteins interact with the β-phosphate of ADP (Story and Steitz, 1992) or GDP (Tong et al., 1991).

The Walker consensus B motif is identified generally by a stretch of four to six hydrophobic amino acids (h) followed by a highly conserved aspartic acid, $(h)_{4-6}$-**D** (Walker et al., 1982; Fry et al., 1986; Hyde et al., 1990;

Mimura et al., 1991). Crystal structures of the recA protein (Story and Steitz, 1992) and bovine F_1-ATPase (Abrahams et al., 1994) indicate that this aspartate also resides within the phosphate binding portion of the ATP-binding pocket. The position of this aspartate in the recA protein suggested a role in coordinating Mg^{2+} (Story and Steitz, 1992; Story et al., 1993). In contrast, no specific role was suggested by the position of this aspartate in F_1-ATPase, and the role of coordinating Mg^{2+} was assigned to a threonine adjacent to the Walker A lysine. Substitution of asparagine (N) for this aspartate in phosphoglycerate kinase reduced ATP binding and enzymatic activity (Minard et al., 1990), and the equivalent substitution in *E. coli* F_1-ATPase reduced the apparent affinities for Mg^{2+} and Mg-ATP and diminished the maximum ATPase activity (Senior and Al-Shawi, 1992). Although the structural and functional studies of these other proteins do not offer a completely coherent picture of the role of the Walker B aspartic acid, the results of the rate analysis for the CFTR mutant D1370N are consistent with a role for this aspartic acid in ATP hydrolysis.

Role of the Invariant Glycine

The functional importance of the invariant glycine in NBF1 (G551) or NBF2 (G1349) is evident from the existence of mutations (G551S, G551D, and G1349D) that are associated with cystic fibrosis in humans (Cutting et al., 1990; Kerem et al., 1990; Strong et al., 1991). However, unlike the residues in the consensus A and B motifs, which are found across families of ATPases and GTPases, the invariant glycine is unique to the traffic ATPase superfamily, for which crystal structures are not yet available. It is therefore more difficult to predict how this residue might contribute to ATP-dependent processes. One view, supported by structural modeling studies of a bacterial permease, His P, suggests that this glycine is part of a linker region that couples the ATP binding pocket to other parts of the protein (Mimura et al., 1991; Shyamala et al., 1991), so substitutions might impair the transduction of conformation changes induced by events in the binding pocket. Another view, suggested by structural modeling of the multidrug resistance protein (Hyde et al., 1990), holds that this glycine is intimately associated with the binding pocket, so substitution might impact directly on the events of ATP binding and or hydrolysis. Support for the latter view is provided by the observation that the mutations G551D and G1349D impair ATP binding in isolated fusion proteins of NBF1 and NBF2, respectively (Logan et al., 1994). On the other hand, the results of Anderson and Welsh (1992) suggested that the mutations G551S and G1349D reduced the open probability of CFTR Cl^- channels without changing the $K_{1/2}$ for the effect of ATP concentration on open probability.

The rate analysis does not pinpoint the function of the invariant glycine, but some potentially important differences between effects of substitutions for the glycine and the consensus A and B residues are apparent. Most striking is the comparison of the effects of substitutions in NBF2 on the deactivation parameters. Replacement of G1349, even by alanine, markedly destabilized the active state, indicated by a dramatic decrease in the latency. In contrast, substitutions for the consensus A lysine (K1250) or the consensus B aspartic acid (D1370) stabilized the active state, as indicated by substantial increases in the latency. In terms of the linker model, this dichotomy could suggest that G1349 is involved in transmitting conformation changes necessary for timing the duration of the active state but does not affect the rate of ATP hydrolysis at NBF2. Alternatively, this glycine could be positioned such that substitution would impair the access of ATP to the binding pocket but not the hydrolysis rate. Yet another possibility is that substitution for this glycine actually increases the rate of ATP hydrolysis at NBF2.

A similar dichotomy was seen in the effects of glycine and binding pocket mutations in NBF1. The most conservative substitution for the glycine (G551A) dramatically attenuated the on rate but tended to stabilize the active state. Substitutions for the binding pocket residues (K464 and D572) also slowed activation, but markedly destabilized the active state. If the glycine functions as part of a linker, then mutations that compromise entry into the active state could also make it more difficult to revert to the inactive conformation. On the other hand, if mutations of the glycine act by obstructing the access of ATP to the binding pocket, this effect could also stabilize the ADP bound state somewhat. An increase in the rate of ATP hydrolysis as a result of glycine mutations in NBF1 seems unlikely, as this would be predicted to increase the activation rate.

Activation and Block of CFTR by IBMX

The goal of these studies was to examine the effects of mutations on the kinetics of transitions between the inactive and active states of the CFTR Cl^- channel. Ideally, this would be done by subjecting the channel to a step increase in the local concentration of the catalytic subunit of protein kinase A. We attempted to approach this ideal in oocytes by using the highest possible concentration of IBMX (5 mM) to maximize the rate and extent of phosphodiesterase inhibition and, hence, the rate of activation of protein kinase A. In addition, concentrations of IBMX above 1 mM are required to achieve significant activation of CFTR mutants such as G551D, D572N, and G1349D (cf. Smit et al., 1993). The use of 5 mM IBMX allowed us to compare insensitive, normal, and hypersensitive mutants on the same basis. The results indicate that mutations in the NBFs

of CFTR can have dramatic effects on the rates of activation and deactivation, as expected if the kinetics of the macroscopic cellular response are dominated by those reflecting transitions of the CFTR protein.

The analysis of the results was complicated somewhat by the fact that 5 mM IBMX produced significant block of the activated CFTR conductance. This effect was particularly noticable following the rapid washout of IBMX, when wild-type CFTR and the hypersensitive mutants exhibited a transient increase in g_{Cl}, consistent with rapid relief of IBMX block. The character of the deactivation following IBMX washout was highly mutant dependent, however, indicating that the dynamics reflected the effects of mutations on the deactivation properties of CFTR. We confirmed this by using forskolin alone to activate CFTR. This is not a satisfactory procedure in general because the response to forskolin alone is absent for insensitive mutants and transient for normal and hypersensitive variants, perhaps because of vigorous phosphodiesterase activity in the oocytes (Sadler and Maller, 1987). It was possible, however, to compare the deactivation of wild-type CFTR and hypersensitive mutants. After washout of 10 μM forskolin, there was no transient increase in g_{Cl}, but the rate of decline was ~fourfold slower for the hypersensitive K1250A mutant, which is consistent with the results seen with 5 mM IBMX. Similar results were obtained by activating with forskolin and 1 mM IBMX. These observations indicate that the procedure used here provides a useful comparison of the dynamics of activation and deactivation for CFTR mutants.

Implications of Macroscopic Rates for Single-Channel Gating

The rate of approach to steady state activation for CFTR-mediated Cl^- conductance was well described by a single exponential. If the gating of CFTR channels were a two-state process, then the values for k_{on} and k_{off} derived from rate analysis would reflect the mean dwell times in the closed and open states of the channel, respectively. Accordingly, a two-state model would predict mean closed times of 1.7 min and open times of about 13 min for wild-type CFTR. Furthermore, the results presented here would predict that both of these dwell times can be dramatically altered by mutations in the nucleotide binding folds.

The gating of CFTR Cl^- channels has been studied in cell-attached and detached membrane patches from a variety of cell types expressing either native or recombinant CFTR. The minimal model that has emerged from such studies would comprise at least two closed states and one open state (Haws et al., 1992; Fischer and Machen, 1994; Venglarik et al., 1994; Winter et al., 1994; Schultz et al., 1995). A simple $C \rightleftharpoons C \rightleftharpoons O$ model can account for the observation that, in an activated steady state, CFTR gating occurs in bursts of rapid openings and closings separated by longer, interburst intervals. Furthermore, Carson et al. (1995) demonstrated in detached patches from transfected HeLa cells or 3T3 fibroblasts that the slow kinetics of steady state CFTR gating, i.e., burst length and interburst interval, are altered by mutations in the NBFs, in a manner that was, in part, consistent with the results presented here. For example, the mutation K1250A increased the burst duration of CFTR by four- to fivefold, and the analysis of CFTR deactivation in oocytes indicates that this substitution produced at least a threefold increase in the stability of the active state (Table II and Fig. 7). Similarly, the mutation K464A increased the interburst interval by fivefold, whereas rate analysis revealed a nearly fourfold slowing of the activation rate (k'_{on}). However, the open probability of K1250A was decreased by more than twofold, largely because of a 30–50-fold increase in the interburst interval, an effect that is not predicted by the present results.

The parallels between the effects of mutations on the activation rate and the single-channel gating are striking, despite the great disparity in the characteristic times of these two processes. The values of burst length and interburst interval observed by Carson et al. (1995) would predict an activation time constant of about 100 ms, whereas the time constant for activation of macroscopic Cl^- conductance in oocytes was ~800-fold slower. This disparity could be, at least in part, a result of the substantial methodologic differences in the two studies. We studied the activation of CFTR by endogenous kinase in oocytes at room temperature (18–20°C), whereas Carson et al. exposed detached membrane patches from mammalian cells to the catalytic subunit of protein kinase A at 34–37°C. In general, however, slower burst kinetics have been observed in on-cell recordings. For example, when CFTR was activated in Calu-3 human airway cells at room temperature using forskolin or isoproterenol (Haws et al., 1994), the mean interburst interval was 38.4 s and the mean open time was 1.8 s, which would predict a time constant for activation of 1.7 s. In oocytes activated using forskolin and 1 mM IBMX, Richards and Dawson (unpublished observations) observed a mean interburst interval of ~16 s and burst lengths of ~1 s, consistent with a time constant for activation of ~1 s.

Despite the considerable variability in the kinetic parameters, the available data suggest that the rates of activation and deactivation of CFTR in oocytes are dominated by processes that are much slower than those which govern the durations of bursts and interburst intervals in the activated steady state. The sensitivity of activation and deactivation to NBF mutations implies that the binding and hydrolysis of ATP are important elements in these slow processes. As regards kinetic states,

the slow processes could represent a long-lived closed state that precedes the bursting state, so that activation and deactivation rates would reflect transitions into and out of the bursting state. Alternatively, the slow processes could represent the progression through a series of closed states, each of which is connected to an open state that is more accessible or more stable than the one preceding.

Some support for the notion of a time-dependent change in burst kinetics can be found in the observations of Fischer and Machen (1994), who studied the time course for activation of wild-type CFTR channels in NIH 3T3 fibroblasts after exposure to forskolin. They found that the open probability increased with a time constant of ~1 min, similar to that observed for the macroscopic conductance in oocytes. The increase in P_o was primarily due to a decrease in the duration of a long closed state over this period. Preliminary observations suggest that a similar process occurs in oocytes; that is, after exposure to forskolin and IBMX, open times increase and interburst intervals decrease with a time course of minutes.

A minimal model for CFTR activation requires phosphorylation of one or more sites on the R domain and the binding and hydrolysis of ATP at one or both of the nucleotide binding folds. The apparent slow step in CFTR activation could reflect dynamics of changes that are initiated by the interaction of the phosphorylated R domain and the NBFs. Other studies have suggested that different phosphorylation states of CFTR have different gating properties. Hwang et al. (1993), for example, defined two different phosphorylation states of CFTR, based on sensitivity to phosphatase inhibitors, and suggested that these two states exhibited differential sensitivity to ATP. Fischer and Machen (1994) also identified high and low P_o states of CFTR that were associated with different levels of stimulation by forskolin. Also, a number of studies (Chang et al., 1993; Rich et al., 1993) have indicated that graded differences in CFTR channel activity can be achieved by the deletion of phosphorylation sites in the R domain or by the permanent deposition of negative charge at these sites. The kinetics of CFTR activation in oocytes may reflect the time dependence of conformational changes that depend on the phosphorylation state of the R domain, which could act to control the gain of ATP-dependent gating processes. The slow kinetics might also reflect the time course of the addition and removal of CFTR channels from the plasma membrane.

Implications for Cystic Fibrosis

The results presented here provide some additional insights into the mechanism by which CFTR mutations produce disease. The conserved glycines in NBF1 (G551) and NBF2 (G1349) are both sites of mutations that cause either mild (G551S) or severe (G551D, G1349D) cystic fibrosis (Smit et al., 1993) but have not been associated with protein processing defects such as those that characterize the ΔF508 mutation. The analysis of activation kinetics presented here strengthens the notion that defects in channel function can cause cystic fibrosis and indicates that the molecular basis for defective function can lie both in the access to and the stability of the activated state. The activation of these mutants, however, suggests that understanding the details of these mechanisms could provide the basis for the design of pharmacologic therapies aimed at amelioration of the symptoms of cystic fibrosis.

We thank Drs. David Gadsby, Tzyh-Chang Hwang, Joseph Metzger, Peter Pedersen, Dorr Dearborn, and Bruce Schultz for stimulating discussions; Dr. Marc Post and James Schafer, Jr., for their help with experiments and data analysis; and John H. Warner for advice on statistical analysis.

This work was supported by grants from the National Institute of Diabetes and Digestive and Kidney Diseases (DK45880, DK29786), the Cystic Fibrosis Foundation, the Howard Hughes Medical Institute, and the University of Michigan G. I. Peptide Center.

Original version received 5 May 1995 and accepted version received 15 September 1995.

REFERENCES

Abrahams, J. P., A. G. W. Leslie, R. Lutter, and J. E. Walker. 1994. Structure at 2.8 Å resolution of F_1-ATPase from bovine heart mitochondria. *Nature.* 370:621–628.

Anderson, M. P., H. A. Berger, D. P. Rich, R. J. Gregory, A. E. Smith, and M. J. Welsh. 1991*a*. Nucleoside triphosphates are required to open the CFTR chloride channel. *Cell.* 67:775–784.

Anderson, M. P., R. J. Gregory, S. Thompson, D. W. Souza, S. Paul, R. C. Mulligan, A. E. Smith, and M. J. Welsh. 1991*b*. Demonstration that CFTR is a chloride channel by alteration of its anion selectivity. *Science.* 253:202–205.

Anderson, M. P., and M. J. Welsh. 1992. Regulation by ATP and ADP of CFTR chloride channels that contain mutant nucleotide-binding domains. *Science.* 257:1701–1704.

Baukrowitz, T., T.-C. Hwang, A. C. Nairn, and D. C. Gadsby. 1994. Coupling of CFTR Cl^- channel gating to an ATP hydrolysis cycle. *Neuron.* 12:473–482.

Bear, C. E., C. Li, N. Kartner, R. J. Bridges, T. J. Jensen, M. Ramjeesingh, and J. R. Riordan. 1992. Purification and functional reconstitution of the cystic fibrosis transmembrane conductance regulator (CFTR). *Cell.* 68:809–818.

Becq, F., M. Fanjul, M. Merten, C. Figarella, E. Hollande, and M. Gola. 1993. Possible regulation of CFTR-chloride channels by membrane-bound phosphatases in pancreatic duct cells. *FEBS Lett.* 327:337–342.

Berger, H. A., M. P. Anderson, R. J. Gregory, S. Thompson, P. W. Howard, R. A. Maurer, R. Mulligan, A. E. Smith, and M. J. Welsh. 1991. Identification and regulation of the cystic fibrosis transmembrane conductance regulator-generated chloride channel. *J. Clin. Invest.* 88:1422–1431.

Carson, M. R., S. M. Travis, and M. J. Welsh. 1995. The two nucleotide-binding domains of cystic fibrosis transmembrane conductance regulator (CFTR) have distinct functions in controlling channel activity. *J. Biol. Chem.* 270:1711–1717.

Carson, M. R., and M. J. Welsh. 1993. 5′-Adenylylimidodiphosphate does not activate CFTR chloride channels in cell-free patches of membrane. *Am. J. Physiol.* 265:L27–L32.

Chang, X.-B., J. A. Tabcharani, Y.-H. Hou, T. J. Jensen, N. Kartner, N. Alon, J. W. Hanrahan, and J. R. Riordan. 1993. Protein kinase A (PKA) still activates CFTR chloride channel after mutagenesis of all 10 PKA consensus phosphorylation sites. *J. Biol. Chem.* 268: 11304–11311.

Cheng, S. H., D. P. Rich, J. Marshall, R. J. Gregory, M. J. Welsh, and A. E. Smith. 1991. Phosphorylation of the R domain by cAMP-dependent protein kinase regulates the CFTR chloride channel. *Cell.* 66:1027–1036.

Coleman, D. E., A. M. Berghuis, E. Lee, M. E. Linder, A. G. Gilman, and S. R. Sprang. 1994. Structures of active conformations of $Gi\alpha_1$ and the mechanism of GTP hydrolysis. *Science.* 265:1405–1412.

Cutting, G. R., L. M. Kasch, B. J. Rosenstein, J. Zielenski, L.-C. Tsui, S. E. Antonarakis, and H. H. Kazazian, Jr. 1990. A cluster of cystic fibrosis mutations in the first nucleotide-binding fold of the cystic fibrosis conductance regulator protein. *Nature.* 346:366–369.

Diamond, G., T. F. Scanlin, M. A. Zasloff, and C. L. Bevins. 1991. A cross-species analysis of the cystic fibrosis transmembrane conductance regulator. Potential functional domains and regulatory sites. *J. Biol. Chem.* 266:22761–22769.

Drumm, M. L., H. A. Pope, W. H. Cliff, J. M. Rommens, S. A. Marvin, L.-C. Tsui, F. S. Collins, R. A. Frizzell, and J. M. Wilson. 1990. Correction of the cystic fibrosis defect *in vitro* by retrovirus-mediated gene transfer. *Cell.* 62:1227–1233.

Drumm, M. L., D. J. Wilkinson, L. S. Smit, R. T. Worrell, T. V. Strong, R. A. Frizzell, D. C. Dawson, and F. S. Collins. 1991. Chloride conductance expressed by ΔF508 and other mutant CFTRs in *Xenopus* oocytes. *Science.* 254:1797–1799.

Fischer, H., and T. E. Machen. 1994. CFTR displays voltage dependence and two gating modes during stimulation. *J. Gen. Physiol.* 104:541–566.

Fry, D. C., S. A. Kuby, and A. S. Mildvan. 1986. ATP-binding site of adenylate kinase: Mechanistic implications of its homology with *ras*-encoded p21, F_1-ATPase, and other nucleotide-binding proteins. *Proc. Natl. Acad. Sci. USA.* 83:907–911.

Gregory, R. J., D. P. Rich, S. H. Cheng, D. W. Souza, S. Paul, P. Manavalan, M. P. Anderson, M. J. Welsh, and A. E. Smith. 1991. Maturation and function of cystic fibrosis transmembrane conductance regulator variants bearing mutations in putative nucleotide-binding domains 1 and 2. *Mol. Cell. Biol.* 11:3886–3893.

Gunderson, K. L., and R. R. Kopito. 1994. Effects of pyrophosphate and nucleotide analogs suggest a role for ATP hydrolysis in cystic fibrosis transmembrane regulator channel gating. *J. Biol. Chem.* 269:19349–19353.

Gunderson, K. L., and R. R. Kopito. 1995. Conformational states of CFTR associated with channel gating: the role of ATP binding and hydrolysis. *Cell.* 82:231–239.

Haws, C., W. E. Finkbeiner, J. H. Widdicombe, and J. J. Wine. 1994. CFTR in Calu-3 human airway cells: channel properties and role in cAMP-activated Cl^- conductance. *Am. J. Physiol.* 266:L502–L512.

Haws, C., M. E. Krouse, Y. Xia, D. C. Gruenert, and J. J. Wine. 1992. CFTR channels in immortalized human airway cells. *Am. J. Physiol.* 263:L692–L707.

Hwang, T.-C., M. Horie, and D. C. Gadsby. 1993. Functionally distinct phospho-forms underlie incremental activation of PKA-regulated Cl^- conductance in mammalian heart. *J. Gen. Physiol.* 101: 629–650.

Hwang, T.-C., G. Nagel, A. C. Nairn, and D. C. Gadsby. 1994. Regulation of the gating of cystic fibrosis transmembrane conductance regulator Cl channels by phosphorylation and ATP hydrolysis. *Proc. Natl. Acad. Sci. USA.* 91:4698–4702.

Hyde, S. C., P. Emsley, M. J. Hartshorn, M. M. Mimmack, U. Gileadi, S. R. Pearce, M. P. Gallagher, D. R. Gill, R. E. Hubbard, and C. F. Higgins. 1990. Structural model of ATP-binding proteins associated with cystic fibrosis, multidrug resistance and bacterial transport. *Nature.* 346:362–365.

Kerem, B.-S., J. Zielenski, D. Markiewicz, D. Bozon, E. Gazit, J. Yahav, D. Kennedy, J. R. Riordan, F. S. Collins, J. M. Rommens, and L.-C. Tsui. 1990. Identification of mutations in regions corresponding to the two putative nucleotide (ATP)-binding folds of the cystic fibrosis gene. *Proc. Natl. Acad. Sci. USA.* 87:8447–8451.

Logan, J., D. Hiestand, P. Daram, Z. Huang, D. D. Muccio, J. Hartman, B. Haley, W. J. Cook, and E. J. Sorcher. 1994. Cystic fibrosis transmembrane conductance regulator mutations that disrupt nucleotide binding. *J. Clin. Invest.* 94:228–236.

Mimura, C. S., S. R. Holbrook, and G. F.-L. Ames. 1991. Structural model of the nucleotide-binding conserved component of periplasmic permeases. *Proc. Natl. Acad. Sci. USA.* 88:84–88.

Minard, P., D. J. Bowen, L. Hall, J. A. Littlechild, and H. C. Watson. 1990. Site-directed mutagenesis of aspartic acid 372 at the ATP binding site of yeast phosphoglycerate kinase: over-expression and characterization of the mutant enzyme. *Protein Eng.* 3:515–521.

Müller, C. W., and G. E. Schulz. 1992. Structure of the complex between adenylate kinase from *Escherichia coli* and the inhibitor Ap_5A refined at 1.9 Å resolution. *J. Mol. Biol.* 224:159–177.

Rich, D. P., H. A. Berger, S. H. Cheng, S. M. Travis, M. Saxena, A. E. Smith, and M. J. Welsh. 1993. Regulation of the cystic fibrosis transmembrane conductance regulator Cl^- channel by negative charge in the R domain. *J. Biol. Chem.* 268:20259–20267.

Riordan, J. R., J. M. Rommens, B.-S. Kerem, N. Alon, R. Rozmahel, Z. Grzelczak, J. Zielenski, S. Lok, N. Plavsic, J.-L. Chou, M. L. Drumm, M. C. Iannuzzi, F. S. Collins, and L.-C. Tsui. 1989. Identification of the cystic fibrosis gene: cloning and characterization of complementary DNA. *Science.* 245:1066–1073.

Sadler, S. E., and J. L. Maller. 1987. *In vivo* regulation of cyclic AMP phosphodiesterase in *Xenopus* oocytes. Stimulation by insulin and insulin-like growth factor 1. *J. Biol. Chem.* 262:10644–10650.

Saraste, M., P. R. Sibbald, and A. Wittinghofer. 1990. The P-loop—a common motif in ATP- and GTP-binding proteins. *Trends Biochem. Sci.* 15:430–434.

Schultz, B. D., R. A. Frizzell, and R. J. Bridges. 1994. IBMX stabilizes the ATP-bound state of ΔF508-CFTR. *J. Gen. Physiol.* 104:35*a*. (Abstr.)

Schultz, B. D., C. J. Venglarik, R. J. Bridges, and R. A. Frizzell. 1995. Regulation of CFTR Cl^- channel gating by ADP and ATP analogues. *J. Gen. Physiol.* 105:329–361.

Senior, A. E., and M. K. Al-Shawi. 1992. Further examination of seventeen mutations in *Escherichia coli* F_1-ATPase β-subunit. *J. Biol. Chem.* 267:21471–21478.

Senior, A. E., S. Wilke-Mounts, and M. K. Al-Shawi. 1993. Lysine 155 in β-subunit is a catalytic residue of *Escherichia coli* F_1 ATPase. *J. Biol. Chem.* 268:6989–6994.

Shyamala, V., V. Baichwal, E. Beall, and G. F.-L. Ames. 1991. Structure function analysis of the histidine permease and comparison with cystic fibrosis mutations. *J. Biol. Chem.* 266:18714–18719.

Smit, L. S., D. J. Wilkinson, M. K. Mansoura, F. S. Collins, and D. C. Dawson. 1993. Functional roles of the nucleotide-binding folds in the activation of the cystic fibrosis transmembrane conductance regulator. *Proc. Natl. Acad. Sci. USA.* 90:9963–9967.

Snedecor, G. W., and W. G. Cochran. 1967. Statistical Methods. 6th edition. Iowa State University Press, Ames, Iowa. 329–330.

Story, R. M., D. K. Bishop, N. Kleckner, and T. A. Steitz. 1993. Structural relationship of bacterial RecA proteins to recombination proteins from bacteriophage T4 and yeast. *Science.* 259: 1892–1896.

Story, R. M., and T. A. Steitz. 1992. Structure of the recA protein-ADP complex. *Nature.* 355:374–376.

Strong, T. V., L. S. Smit, S. V. Turpin, J. L. Cole, C. T. Hon, D. Markiewicz, T. L. Petty, M. W. Craig, E. C. Rosenow III, L.-C. Tsui, M. C. Iannuzzi, M. R. Knowles, and F. S. Collins. 1991. Cystic fibrosis gene mutation in two sisters with mild disease and normal sweat electrolyte levels. *N. Engl. J. Med.* 325:1630–1634.

Sung, P., D. Higgins, L. Prakash, and S. Prakash. 1988. Mutation of lysine-48 to arginine in the yeast RAD3 protein abolishes its ATPase and DNA helicase activities but not the ability to bind ATP. *EMBO J.* 7:3263–3269.

Tabcharani, J. A., X.-B. Chang, J. R. Riordan, and J. W. Hanrahan. 1991. Phosphorylation-regulated Cl^- channel in CHO cells stably expressing the cystic fibrosis gene. *Nature.* 352:628–631.

Thiagalingam, S., and L. Grossman. 1991. Both ATPase sites of *Escherichia coli* UvrA have functional roles in nucleotide excision repair. *J. Biol. Chem.* 266:11395–11403.

Tong, L., A. M. de Vos, M. V. Milburn, and S.-H. Kim. 1991. Crystal structures at 2.2 Å resolution of the catalytic domains of normal *ras* protein and an oncogenic mutant complexed with GDP. *J. Mol. Biol.* 217:503–516.

Tucker, S. J., D. Tannahill, and C. F. Higgins. 1992. Identification and developmental expression of the *Xenopus laevis* cystic fibrosis transmembrane conductance regulator gene. *Hum. Mol. Genet.* 1: 77–82.

Venglarik, C. J., B. D. Schultz, R. A. Frizzell, and R. J. Bridges. 1994. ATP alters current fluctuations of cystic fibrosis transmembrane conductance regulator: evidence for a three-state activation mechanism. *J. Gen. Physiol.* 104:123–146.

Walker, J. E., M. Saraste, M. J. Runswick, and N. J. Gay. 1982. Distantly related sequences in the α- and β-subunits of ATP synthase, myosin, kinases, and other ATP-requiring enzymes and a common nucleotide binding fold. *EMBO J.* 1:945–951.

Wilkinson, D. J., M. K. Mansoura, P. Y. Watson, L. S. Smit, F.S. Collins, and D. C. Dawson. 1994. CFTR activation: distinct roles for the nucleotide binding folds. *J. Gen. Physiol.* 104:34*a.* (Abstr.)

Wilkinson, D. J., L. S. Smit, M. K. Mansoura, F. S. Collins, and D. C. Dawson. 1993. Activation and deactivation of CFTR Cl^- conductance: differential effects of analogous mutations in NBF1 and NBF2. *Pediatr. Pulmonol.* S9:205.

Winter, M. C., D. N. Sheppard, M. R. Carson, and M. J. Welsh. 1994. Effect of ATP concentration on CFTR Cl^- channels: a kinetic analysis of channel regulation. *Biophys. J.* 66:1398–1403.